REPORT DOCUMENTATION PAGE

AFRL-SR-AR-TR-05-

0343

1. REPORT DATE *(DD-MM-YYYY)*	2. REPORT TYPE	3. DATES COVERED *(From - To)*
4/29/2005	Final Performance Report	5/1/2002 - 2/2/2005

4. TITLE AND SUBTITLE

Anharmonic and Standing Dynamo Waves: Theory and Observation of Stellar Magnetic Activity (Final Report to AFOSR Grant F49620-02-1-0194 entitled "From Space Weather, Space Climate to Terrestrial Climate: Physical Constraints from Minutes, Millenia to Millions of Years Through Observations of the Sun and Sun-Like Stars)

5a. CONTRACT NUMBER
F49620-02-1-0194

5b. GRANT NUMBER
N/A

5c. PROGRAM ELEMENT NUMBER
N/A

6. AUTHOR(S)

S. Baliunas, P. Frick. D. Moss, E. Popova, D. Sokoloff, and W. Soon

5d. PROJECT NUMBER
N/A

5e. TASK NUMBER
N/A

5f. WORK UNIT NUMBER
N/A

7. PERFORMING ORGANIZATION NAME(S) AND ADDRESS(ES)

Harvard-Smithsonian Center for Astrophysics
60 Garden Street
Cambridge, MA 02138

8. PERFORMING ORGANIZATION REPORT NUMBER
N/A

9. SPONSORING/MONITORING AGENCY NAME(S) AND ADDRESS(ES)

Mount Wilson Institute
P.O. Box 1909
Atlanta, GA 30301-1909

NM

10. SPONSOR/MONITOR'S ACRONYM(S)
MWI

11. SPONSOR/MONITOR'S REPORT NUMBER(S)
N/A

12. DISTRIBUTION/AVAILABILITY STATEMENT

Approved for public release; distribution is unlimited

20050901 066

13. SUPPLEMENTARY NOTES

The results of this study have been submitted for publication in the Monthly Notices of the Royal Astronomical Society

14. ABSTRACT

The familiar decadal cycle of solar activity is one expression of interannual variability of surface magnetism observed in stars on or near the lower main sequence. Records of Ca II H and K fluxes obtained for such stars by Mount Wilson Observatory's HK Project extend back over 35 years. From thesese records, we define a new measure of anharmonicity that connects to the 2-D description of a Parker dynamo model. We explore the parameter space of this model and find an excellent counterpart to solutions containing highly anharmonic, standing dynamo waves in the records of several of the lowest mass (late K- to early M-type) active stars in the sample. We interpret anharmonicity as resulting from non-propagating or standing dynamo waves, which operate in a substantially supercriticial regime. There, for most of the cycle, large-scale magnetic fields are generated and maintained by winding of field by differential rotation rather than by joint action of differential rotation and helical convection. Further, less active stars like the Sun show simple harmonic, migratory and/or intermediate-type dynamo wave patterns over a broad range of dynamo parameters

15. SUBJECT TERMS

stars: rotation; late-type; magnetic fields; chromospheres; activity

16. SECURITY CLASSIFICATION OF:			17. LIMITATION OF ABSTRACT	18. NUMBER OF PAGES	19a. NAME OF RESPONSIBLE PERSON
a. REPORT	b. ABSTRACT	c. THIS PAGE			Harold A. McAlister
U	U	U	UU	33	19b. TELEPHONE NUMBER *(Include area code)* 404-651-2932

ABSTRACT

The familiar decadal cycle of solar activity is one expression of interannual variability of surface magnetism observed in stars on or near the lower main sequence. From studies of time series of Ca II H and K emission fluxes that go back more than 35 years and have been accumulated for such stars at the Mount Wilson Observatory (MWO) by the HK Project, we define a quantitative measure, called anharmonicity, of the cyclic component of interannual magnetic variability. Anharmonicity provides a connection between observed variations in magnetic activity and the two-dimensional description of a Parker dynamo model. We explore the parameter space of the Parker dynamo model and find an excellent counterpart to the solutions containing highly anharmonic, standing dynamo waves in the records of several of the lowest-mass (late K- to early M-type) active stars in the HK Project sample. We interpret anharmonicity apparent in the records as resulting from non-propagating or standing dynamo waves, which operate in a regime that is substantially supercriticial. There, for the majority of a cycle or pulse of decadal-to-interdecadal variability, the large-scale magnetic fields are generated and maintained by winding of field by differential rotation rather than by the joint action of differential rotation and helical convection. Among the less active stars (the Sun is considered such a star in the HK Project sample) we find a correspondence between anharmonicity and Parker dynamo model solutions that include simple harmonic, migratory and/or intermediate-type dynamo wave patterns over a broad range of dynamo parameters.

Subject headings: stars: rotation — stars: convection — stars: magnetism — stars: chromospheres

1. Introduction

Four decades ago astronomers found evidence that main sequence stars with non-negligible subsurface convective zones display surface magnetism similar to that seen on the Sun (Wilson 1963; Kraft 1967). Modern works attempting to delimit the occurence of surface magnetism of main sequence stars find its onset below a mass of approximately 1.5 solar masses (Suchkov et al. 2003), and it persists even to very low mass, fully convective stars at the far end of the M-dwarf spectral sequence (Mohanty & Basri 2003).

In the only program of its kind, the surface magnetic activity of over 3000 stars has been monitored at Mount Wilson Observatory (MWO) as the HK Project, with approximately one hundred stars on or near the lower main sequence having been monitored for as long as 38 years. The program makes use of the inference of surface magnetism by proxy from the fluxes of the emission cores at the centers of the singly-ionized calcium H (396.8 nm) and K (393.4 nm) spectrum lines (Fawzy et al. 2002a,b). On the Sun the fluxes in the narrow emission cores (with a full width of $\sim$0.1 nm at their bases) have been found to be excellent indicators of magnetic activity. An increase in either or both the magnetic field strength of, or coverage by, surface features increases the disk-integrated Ca II flux; the observed, integrated response over the period of the sunspot cycle is approximately linear. Thus, while the surfaces of other solar-like stars are not resolved by even the largest existing telescopes, monitoring of the Ca II flux yields information on starspots and other surface features that are sub-hemispheric in size (Wilson 1978; Baliunas et al. 1995). These works found the decadal cycle of surface magnetism seen on the Sun to be one class of interannual variability observed in the HK Project sample. While some records showed cycles similar to appearance to the sunspot cycle, other records showed more complex variability not readily classified as cyclic, and still others little variability, as defined by the system sensitivity.

The origin of interannual magnetic variability is thought to be associated with dynamo

action that occurs within the subsurface convective zone, or near it in the overshoot layer, which then produces large-scale dynamo waves that in principle can have various characteristics, e.g. propagating or standing. However, stellar dynamo theory is far from being able to deduce dynamo related quantities from comparison between its results and those of observations. One reason is that the magnetic proxies – time series of emission fluxes – give only a one-dimensional representation of stellar activity, while even the simplest model of the stellar dynamo, the so-called Parker dynamo, contains a two-dimensional description, with activity waves propagating from middle latitudes towards the equator, in the case of the Sun. Reconstruction of a two-dimensional distribution of magnetic features from one-dimensional proxies is far from straightforward (Strassmeier 2005).

Here we invoke a parameter that describes the form or shape of the cyclic component that may be present in the observed records of interannual variability. The parameter, called anharmonicity, appears to be associated with the spatial configuration of the dynamo wave. The suggestion is based on the following property of the Parker dynamo. In a prescribed velocity field, the kinematic dynamo produces harmonic activity waves with amplitudes that grow exponentially in time. More realistic (nonlinear) dynamos introduce some mechanism of dynamo quenching to obtain a steady activity cycle with finite magnetic field strength, such as seen for the Sun. The temporal shape of the quenched cycle can be quite far from harmonic. Moss et al. (2004) suggested that the degree of anharmonicity of cyclic component of interannular activity generated by a dynamo could be a useful source of information about parameters governing dynamo generation of magnetic field. For example, Moss et al. demonstrated that the structure of butterfly diagrams for almost harmonic interannual variability differs physically from that corresponding to strongly anharmonic variability. The former displays activity waves propagating from middle latitudes towards the stellar equator, while the latter is represented by (almost) standing activity waves. We start with a qualitative explanation of this result from stellar dynamo theory (Section 2).

The next question is whether the available data allow a distinction between (almost) harmonic and strongly anharmonic cycles. In Section 3, we argue that the Double Wavelet Analysis (DWA) method developed in Soon et al. (1999) and Frick et al. (2004) provides such a possibility. Preliminary results in this direction have been presented in conference proceedings (Baliunas et al. 2004).

We show (Section 3) how we estimate the anharmonicity of the cyclic interannual variability seen in several records of proxy surface magnetism from the HK Project selected for this initial study. We then use the same algorithm to calculate the anharmonicity for the Parker dynamo solutions (Section 4) for various values of the governing parameters (see e.g. Table 2). Tests are further conducted to assess limitation and robustness of our DWA-derived anharmonicity in Section 4.

As a result, we suggest that the anharmonic interannual variability seen in some stars can be associated with a physical mechanism that apparently is not expressed in the Sun. In addition to the conventional picture of propagating waves that produce interannual magnetic variability, we find that in some stars this magnetic activity can be associated with almost standing, anharmonic dynamo waves. In Section 5 we examine a list of stars whose records of interannual variability seem promising in terms of this new interpretation.

Taking into account that the activity records pertain to a disk-integrated description of stellar surface magnetism, we restrict our theoretical analysis by adopting the simplest two-dimensional – in time and latitude – representation of the Parker dynamo model. We should remember that a more detailed analysis that uses two or even three spatial dimensions, and a more realistic description of stellar internal rotation could alter our interpretation. To explore this possibility, we discuss in Section 6 information from other approaches to the topic.

2. Standing anharmonic dynamo waves

The theoretical idea behind the occurence of standing dynamo waves is connected to the fact that the stellar dynamo is a threshold phenomenon. It seems quite clear that, provided a stellar dynamo is marginally excited, the dynamo wave is expected to be almost sinusoidal. In contrast, if the dynamo action is highly supercritical, the dynamo wave can be substantially anharmonic. We show below that such a highly anharmonic dynamo wave may become almost a standing wave in certain regimes of dynamo parameters.

The mean-field dynamo equations (e.g. Krause & Rädler 1980) governing magnetic field generation in a thin convective shell can be reduced to the form

$$\frac{\partial B}{\partial t} = Dg \sin\theta \frac{\partial A}{\partial \theta} + \frac{\partial^2 B}{\partial \theta^2} + \tilde{\mu}^2 \frac{\partial^2 B}{\partial r^2}\,, \tag{1}$$

$$\frac{\partial A}{\partial t} = \alpha B + \frac{\partial^2 A}{\partial \theta^2} + \tilde{\mu}^2 \frac{\partial^2 A}{\partial r^2}\,. \tag{2}$$

Here B is the toroidal magnetic field measured in units of the equipartition field $B_{\rm eq}$, A is the toroidal component of the vector potential responsible for the poloidal magnetic field and θ is colatitude ($\theta = 0$ corresponds to the north pole). The equations are presented in a dimensionless form, so the latitudinal diffusion is incorporated into the dynamo number D and the radial diffusion is represented by the coefficient $\tilde{\mu}^2$, $\tilde{\mu} \sim R/s$, where R is the stellar radius and s is the thickness of the convective zone. A factor $g(r,\theta)$ has been introduced to represent the rotation curve. Eqs. (1) and (2) neglect the curvature of the convective shell and also replace the magnetic field behaviour near the stellar poles by the requirement that the magnetic field vanishes at the boundaries of the domain $-\Theta^* \le |\theta - \pi/2| \le \Theta^*$ in which dynamo generation is assumed to occur; in the computations of Moss et al. (2004) $\Theta^* = \pi/2$. See Galitsky & Sokoloff (1999) for the incorporation of a more realistic description of the polar regions into this model.

Parker (1955) averaged Eqs. (1) and (2) with respect to r and replaced the terms with

r-derivatives by decay terms to get the equations

$$\frac{\partial B}{\partial t} = gD\sin\theta\frac{\partial A}{\partial \theta} + \frac{\partial^2 B}{\partial \theta^2} - \mu^2 B, \tag{3}$$

$$\frac{\partial A}{\partial t} = \alpha B + \frac{\partial^2 A}{\partial \theta^2} - \mu^2 A. \tag{4}$$

He pointed out that the terms responsible for radial diffusion can be incorporated into the left hand sides of Eqs. (3) and (4) provided that the kinematic dynamo problem is being considered. Now $g = g(\theta)$ in general; we consider the simplest case $g = 1$. For the homogeneous case, i.e. for α independent of θ, a growing eigensolution is present provided that $|D|$ is large enough, $|D|^{1/3} \geq O(\mu)$. If $|D|^{1/3} \approx \mu$ then the dynamo wavelength is comparable with the shell thickness, while for $|D|^{1/3} \gg \mu$ the wavelength is much shorter than the shell thickness.

The term responsible for the radial diffusion plays a very important role in the nonlinear case. When there is no explicit latitudinal dependence of helicity, $\alpha = \alpha(B)$, and $|D|^{1/3} \sim \mu$, the wavelength of the stationary dynamo wave is determined by the shell thickness. The wave remains short if α varies smoothly, a solution found by Meunier et al. (1997) and Bassom et al. (1999). The situation is quite different if $|D|^{1/3} \gg \mu$, i.e. if μ is a constant which can be small, but fixed and independent of $|D|$, which is presumed to tend to infinity. For the spatially homogeneous case, the stationary dynamo waves appear as long waves, with length comparable to the shell length, i.e. πR, where R is the shell radius.

It is clear that $R > s$ so that μ cannot be arbitrary small. If, however, $|D|^{1/3} \gg \mu$, diffusive losses are determined by latitudinal diffusion and the terms containing μ can be neglected, so one can formally set $\mu = 0$.

Moss et al. (2004) numerically investigated Eqs. (3) and (4) for large (and negative)

values of D, $10^2 \leq |D| \leq 10^6$, $0 \leq \mu \leq 10$ and a simple algebraic nonlinearity

$$\alpha(B) \propto f(B)\cos\theta, \qquad f(B) = 1/(1+B^2). \tag{5}$$

This range contains values which seem to correspond to the solar convective shell (with, e.g. $D = -10^3$ and $\mu = 3$ crudely representing a convective shell with radial extent about 1/3 of the solar radius). It was found that the case $|D|^{1/3} \approx \mu$ is associated with an almost harmonic shape of the dynamo wave while the case $|D|^{1/3} \gg \mu$ gives quite anharmonic waves. The harmonic wave propagates from the middle latitudes equatorwards. The direction of the wave propagation is determined by the sign of $g\alpha$; this results from a standard linear analysis of Eqs. (3) and (4) by Parker (1955). That analysis remains applicable for a moderately supercritical situation because a moderate suppression of α still provides a stable propagating dynamo wave.

The situation becomes quite different when the dynamo becomes highly supercritical, i.e. for $|D|^{1/3} \gg \mu$. In order to prevent an unbounded growth of magnetic field, α must be substantially suppressed so that B becomes much larger than in weakly nonlinear solutions. Because α is highly suppressed ($B >> B_{\rm eq}$), $\alpha \approx 0$ during the major part of the cycle, so that the magnetic field is simply wound up by differential rotation. Importantly, this winding does not select any direction of dynamo wave propagation, and the wave becomes a standing wave throughout most phases of the cycle. It is only during the brief phase, near the instant of magnetic dipole reversal when the toroidal field is weak, that the α-effect becomes substantial enough to participate in the magnetic field evolution. During this brief phase of the activity cycle, the dynamo wave propagates like a harmonic wave. Such a two-stage cycle is thus highly anharmonic. The numerical studies of Moss et al. (2004) support this interpretation. Note that although the α-effect is important only for a small part of the cycle, its role is vital – winding up of the field by differential rotation alone cannot maintain a large-scale magnetic field.

Both regimes described above, i.e. that with a harmonic, propagating wave as well as that of an (almost) standing anharmonic wave, could be relevant to lower-main sequence stars, which display interannual variability sometimes very different in form from the sunspot cycle. The one-dimensionality of the observations do not allow direct distinction between standing and harmonic waves, in the absence of the explicit construction of a butterfly diagram. We thus propose to isolate the two distinct dynamo wave patterns by searching for relatively anharmonic cycles and assuming them to be associated with standing activity waves.

Fig. 1 summarizes the general behavior of the dynamo wave solutions as functions of μ and D taking the α-quenching given by Eq. (5).

3. Measuring the anharmonicity

The observed records of surface magnetism for five stars with different patterns of interannual variability are shown in Fig. 2, which add to the list of stars previously studied in Frick et al. (2004) and Baliunas et al. (2004). The signals are obviously not strictly harmonic. We now introduce a quantitative measure for their anharmonicity.

One straightforward quantity related to the anharmonicity of stellar cycles is the ratio of the second to the first harmonic (M_2/M_1) in the Fourier spectra of the observed time series. The values of M_2/M_1 for several HK-project stars (which were previously studied in Frick et al. 2004 but with anharmonicity results not yet presented), calculated using the conventional Fourier transform are given in the last column of Table 1.

However, the applicability of Fourier analysis to noisy records – that is, records containing variability on several timescales – is limited if not biasing. We thus introduce a less biasing method, based on the wavelet transform, to calculate anharmonicity. Wavelets

have become a common instrument for analysis of time signals with complicated structure, including the presence of multiperiodic, non-stable frequencies, noisy, multi-scale time features, etc. Wavelets provide a powerful capability to identify isolated, cyclic features within a record, to follow the variability of the frequency (period) of a cyclic process, to localize or accurately resolve some short pulses in the time domain, and to filter noise at particular frequencies.

In our analysis we use the Morlet wavelet $\psi(t) = \exp(-t^2/2\kappa^2 + i2\pi t)$, with an adjustable parameter, κ, which can be fine-tuned to yield optimal resolutions of time and frequency. In this case, the resolutions of the wavelet for a given characteristic time-scale, T, are $\delta t = c\kappa T$, $\delta\omega = c/(\kappa T)$, where c is a constant of order unity. Smaller values of κ give better time resolution (δt), while larger values of κ improve frequency resolution ($\delta\omega$). A more sophisticated analysis of the wavelet plane can be performed by reusing the wavelets themselves, as in the so-called Double Wavelet Analysis, or DWA, introduced by Soon, Frick & Baliunas (1999) and Frick et al. (2004), for an accurate determination of the frequency corresponding to the stellar rotation period.

To illustrate the basic principle of DWA, we start with the wavelet transform of the signal $f(t)$, giving the wavelet coefficients $W_1(a,t) = a^{-1/2} \int f(t')\Psi((t'-t)/a)dt'$. Using the Morlet wavelet with good spectral resolution ($\kappa = 4$) we compute the wavelet spectrum $E_1(a) = \int |W_1(a,t)|^2 da$, and seek a periodicity (P_c) on a timescale of years, which would correspond to the activity cycle. Then we take the second wavelet transform for each time-scale a using only one scale parameter, set to be the cycle length, P_c. Next, we consider the modulus of the wavelet coefficients and determine

$$W_2(a,t) = a^{-1/2} \int |W_1(a,t')| \Psi(\frac{t'-t}{P_c}) dt'.$$

Finally, we obtain the DWA spectrum $E_2(a) = \int |W_2(a,t)|^2 \, da$.

The goal of the procedure is to find the scale a^* in the DWA spectrum that gives the maximal power at the scale that corresponds to the predominant frequency which is now referred to as the activity cycle length, P_c. The ratio $A = P_c/a^*$ provides a measure of the characteristic of "anharmonicity" of the cyclic component of interannual magnetic variability in terms of the integrated wavelet power concentration at the original frequency.

We have tested the procedure above by calculating the anharmonicity of a sequence of synthetic test signals (Baliunas et al. 2004) to confirm that A gives a reasonable estimate of anharmonicity.

4. Anharmonicity of observed and simulated dynamo waves

We apply the DWA method to calculate the value A for the stars listed in Table 1. The stars in Table 1 were originally chosen in Frick et al. (2004) for a previous application and exploration of our Double Wavelet Analysis (DWA) method to study rotation-modulated signals. Two more stars, young and relatively active, HD 18256 and HD 20630, were added subsequent to Frick et al. (2004); preliminary results for all stars in Table 1 were reported in Baliunas et al. (2004).

In this paper we explore examples of highly anharmonic cycles, as indicated from the observed records of stellar activity with results from models of the theoretical Parker migratory dynamo. For this purpose, we have chosen a new set of stars that whose observed records of surface magnetism shown in Fig. 2; the selection criteria of stars with larger values of A (regimes of low μ and high D) is next established. As a foreshadowing of our results (Section 5), we do find examples of travelling and standing dynamo waves in the records of the selected stars.

Moss et al. (2004) investigated numerically Eqs. (3) and (4) for large and negative

values of $|D|$, $10^3 \leq |D| \leq 10^6$ and a range of μ values with $0 \leq \mu \leq 10$ (see Moss et al. (2004) for details of the model). Several typical time series produced by the model solutions are shown in Fig. 3; deviations from harmonic cycle behaviour are easily recognizable by eye. We calculated anharmonicity measures for the magnetic fields of these dynamo model solutions taken at an arbitrarily chosen latitude ($\theta = \pi/4$), and present the results in Table 2.

Comparing Tables 1 and 2, we conclude that the range in anharmonicity obtained from the observational data is reasonably close to that from our simple dynamo models, as previously reported in Baliunas et al. (2004). The two active and younger stars, HD 18256 and HD 20630, exhibit particularly anharmonic activity cycles. The question next to be clarified is how robust are the anharmonicity measures under the potential influence of observational biases? Wavelet transform results have been proven to be robust under perturbations by random noise, whose presence is inevitable in any observational time series. We have presented several tests under random noise perturbation scenarios in our previous papers (see e.g., Frick et al. 1997). Here, however, we must deal with the possibility of more specific and critical observational biases.

The sensitivity or robustness tests we wish to investigate for our DWA measure of anharmonicty are related to the fact that our one-dimensional integrated Ca II surface emission fluxes necessarily include signals from an integrated stellar hemisphere. In the case where the stellar rotation axis is perpendicular to our line of sight, the signal is integrated over the north and south hemispheres. In contrast, simulated dynamo model signals are obtained for a prescribed dipole symmetry about the equator. But the spatial symmetry in reality will probably be imperfect: the activity cycles in the Sun's Northern and Southern hemispheres can be substantially displaced in time. This time displacement can be represented as an admixture of a quadrupole with a dipole mode (Sokoloff &

Nesme-Ribes 1994). Thus, a finite phase displacement between unresolved contributions from northern and southern hemispheres may contaminate the deduced anharmonicity measure from either DWA or the Fourier harmonic ratio. A similar bias doubtless exists in the observed stellar Ca II activity records. We now investigate the robustness of the anharmonicity measures for this specific bias.

We address the problem as follows. Let $f(t)$ be a signal taken from a numerical dynamo simulation, as described above, for one hemisphere. We mimic the potential hemispheric bias introducing a phase-shifted signal

$$F_{c,\tau}(t) = f(t) + cf(t+\tau)\,. \tag{6}$$

Here τ is a displacement of the cycle in one hemisphere relative to the other. We measure τ in units of the activity cycle P_c; and the adjustable parameter c allows for the fact that the cycle amplitude may differ between hemispheres. The anharmonicity measure will be robust against north-south asymmetry bias if for $f(t)$ and $F_{c,\tau}(t)$ results are close to each other in both the original and shifted series.

Of course, it would be a miracle to get robust results for all values of c and τ. In our sensitivity tests the value of A is robust for $\tau \leq 0.2$ (i.e. a relative displacement of up to 20%) and $c \leq 1.5$ (i.e. an intensity contrast of up to 50%). We illustrate the sensitivity test results in Table 3 for some arbitrarily chosen combinations of D and μ values.

We conclude that the values of A are fairly robust for most cases presented up to values $\tau = 0.2$, and in some cases even for a slightly larger τ (up to 25%). The values of A for the particular case of $D/D_\odot = 1000$, $\mu/\mu_\odot = 0.5$ look less robust when compared to other cases. But the stellar activity cycle generated for this case is so far from harmonic that the cycles cannot be properly defined (i.e. the Parker dynamo is operating in the highly supercritical magnetic field regime – Moss et al. 2004). The fact that the calculated values

of A are so extremely high in this case is sufficient hint of a poorly defined activity cycle.

We learn from Table 3 that the other measure of anharmonicity, M_2/M_1, is much less robust with respect to hemispheric timing bias (although M_2/M_1 seems robust in narrower circumstances, namely $\tau \leq 0.1$). Thus we adopt A as our anharmonicity measure.

We now proceed to associate two-dimensional information with the observational records by way of the dynamo models. We classify the anharmonicity data listed in Table 2 as corresponding to migratory or standing butterfly diagrams, relying on Fig. 10a of Moss et al. (2004), to obtain Table 4 where dynamo waves are broadly presented as migratory (M) and standing (SW) for various values of D and μ. The problem to note here is that the transition between migratory and standing waves is generally smooth and gradual, so any sharp demarcation into classes is somewhat subjective (Moss et al. 2004). This is why we have added an additional category, "intermediate" (I), for the dynamo wave patterns indicated in Table 4. There are solutions with small μ for which the butterfly diagrams look almost like a stationary pattern; that is, there is no real migration. For larger values of μ, there are sometimes solutions which have a very box-like (or rectangular) form, but which also show almost no migration. In Table 4, we classified both these cases as "I". For the clearly migratory solutions, the contours in the latitude-time plane are very flattened ellipses.

We conclude from a comparison of Tables 2 and 4 that the value of the anharmonicity A is related to the migration properties of the activity wave. Dynamo waves with harmonic cycles (relatively small A) are migratory while the strongly anharmonic cycles with larger values of A are largely associated with standing waves. The threshold anharmonicity value for standing waves is somewhere near $A = 1.5$. Realizing that the anharmonicity measure A can be indistinct or poorly determined and that some stars will show cycles with $A \approx 1.5$, we avoid any definitive interpretation concerning a migratory or standing nature of such

stellar activity dynamo waves. If, however, the value of A substantially exceeds 1.5, the dynamo wave can be suspected to be of standing type. For values of A substantially lower than 1.5, a migratory dynamo wave is indicated.

We conclude that the quantity A as a measure of anharmonicity seems perhaps not very sensitive to the inter-hemispheric timing bias. Through the creation of sets of artificial signals, a more sensitive measure of the anharmonicity issue could perhaps be produced. We prefer, however, to be cautious for now and to use our possibly less sensitive, although relatively robust, measure of anharmonicity.

5. Stars where standing activity waves are suspected

Results from Table 1 suggest a possibility of finding standing dynamo waves in the two active stars, HD 18256 and HD 20630, which have high DWA anharmonicity values of $A = 3.8$ and 2.9, respectively. Motivated further by the robust qualitative results presented in Table 4 and Fig. 1 that indicate standing dynamo wave solutions in the regimes of low μ and high D, that is for larger values of A, we examined additional records of the HK Project. We selected five more active, late-type stars with spectral type later than G7 for this purpose: HD 131165A (G8V), HD 131165B (K4V), HD 201091 (K5V), HD 201092 (K7V) and HD 95735 (M2.1Ve) (see Fig. 2). The first four stars are actually two pairs of well-resolved visual binaries whose components stars are each of mass small enough to possess an extensive, outer convective envelope. The last star chosen is the coolest star in the long-term monitoring program of the HK Project, and its fully convective envelope is not dissimilar to those of the dMe flare stars. Although not known as a flare star, HD 95735 flared spectacularly in 1981 during routine observations, when the Ca II H and K S-index value shot up by 300-400% from its interannual mean and then decayed as monitoring continued over a 2-hour period (Donahue et al. 1986).

5.1. HD 201091 and HD 201092

Activity cycles as well as rotation cycles are readily recognized by eye for both companions of this binary system (Figs. 4a and 4b). According to the ordinary wavelet spectra the activity cycle of HD 201091 is $P_c = 2740$ days, the rotation period is about 44 days, while our DWA analysis gives $P_r = 47.5$ days for the rotation period; an additional significant peak at 5.3 days also appears. We associate this additional peak with the influence of the companion but any further interpretation would require detailed mechanistic modeling as mentioned earlier in Frick et al. (2004). The anharmonicity $A = 1.38$ (the peak from DWA analysis gives $P_c = 1982$ days), and so we may interpret the activity cycle in HD 201091 as a migrating activity wave.

For HD 201092, the activity cycle is identified by the peak at $P_c = 4260$ days. The rotation period $P_r = 45$ days according to the ordinary wavelet spectra, and $P_r = 51$ days according to the DWA spectra. We note that the rotation periods for both companions are similar enough to suggest the rotation of binaries could be synchronized by tidal interactions, but the orbital period of HD 201091/201092 system is about 653 years. The more likely interpretation appears to be that both stars have identical ages, and are close enough in mass for their rotation periods to be similar. (Before our study of DWA spectra, no such interpretation about the rotation periods of the two stars was even possible.) For HD 201092, we obtain $A = 3.8$ (the peak from DWA analysis gives $P_c = 4260$ days) which suggests a highly anharmonic, standing activity wave.

Thus, for nearly the last four decades, the dynamo operating in these two, presumably coeval stars that are also close in mass, has expressed different patterns: HD 201092 seems a good candidate for possessing standing magnetic activity wave while its companion, HD 201091, seems to display a conventional, or Sun-like, migrating activity wave.

5.2. HD 131156A and HD 131156B

The activity cycle period for HD 131156A is assumed to be given approximately by $P_c = 4807$ days, and the DWA analysis suggested the cycle-related a-scale, $a^* = 1760$ days (Fig. 5a), so that the value of anharmonicity is $A = 2.7$. The rotation period is estimated to be $P_r = 8.2$ days from the wavelet spectrum; however, that frequency is not very pronounced in the DWA spectrum.

The activity cycle in HD131156 B looks weak (Fig. 5b) and prevents any justifiable statement concerning the configuration of its dynamo activity wave.

HD 131156A appears to be another good candidate for the presence of standing dynamo wave activity, but this case is not as obvious as for HD 201092.

5.3. HD 95735

The results for HD 95735 are complicated (Fig. 6). Supposing $P_c = 4120$ days to be the approximate time-scale for the poorly defined activity cycle, we obtain from the DWA analysis the value of the cycle-related a-scale to be as low as $a^* \approx 832$ days. This makes the anharmonicity value $A = 4.9$. We note a very strong peak in the DWA spectrum at $P_r = 28.5$ days, which could be identified with axial rotation; however, no pronounced peak is apparent in the ordinary wavelet spectrum. We note also a third peak in the DWA spectrum at 4.5 days. We conclude that HD 95735 hints of standing wave activity but its almost fully convective outer envelope could be indicative of a more random and irregular magnetic field activity on its surface, generated and maintained by something like a distributed dynamo (see e.g. Covas, Moss & Tavakol 2005) or a small-scale dynamo that requires an intensive turbulent fluid motion possessing helicity (see e.g. Zeldovich, Ruzmaikin & Sokoloff 1990; Schekochihin et al. 2004).

6. Conclusion and discussion

We have suggested a measure, called anharmonicity, of the interannual variability of surface magnetism seen in records of stars on or near the lower main sequence. For five stars whose records spanning nearly four decades from the Mount Wilson Observatory's HK Project, we have identified and studied the differences between the almost-harmonic and substantially-anharmonic cycles. Study of the nonlinear Parker dynamo models associate the highly anharmonic activity cycles with (almost) standing activity waves, rather than travelling waves. We appreciate that this conclusion is predicted on the basis of a very simple model of stellar magnetic activity, i.e. the Parker dynamo. In this interpretation, the physical reason for the standing wave is an effective suppression of the α-effect during the major part of the activity cycle, which is expected when the stellar dynamo is substantially supercritical. In this situation, the magnetic field is subjected solely to winding up by differential rotation, rather than the joint action of differential rotation and helical convection. The winding up does not determine a direction of propagation, so the wave becomes a standing wave. This physical effect may also apply to more sophisticated and realistic stellar dynamo models; thus, we expect that a more realistic dynamo model will still yield magnetic activity cycles associated with standing waves.

Are standing activity waves possible in other physical circumstances?

Standing-wave magnetic patterns are expected by dynamo theory in some close binaries (Moss, Piskunov & Sokoloff 2002). An area of enchanced dynamo activity may be expected in such cases because of the reflection effect in a close binary system, which in turn leads to a mutual heating of a limited surface sector for both companions of a binary system. If the heating and associated modification of stellar convection are strong or powerful enough to affect or feed back on the internal dynamo action, then nonaxisymmetric structures anchored to the regions where additional heating occurs may be excited. This example

is interesting for our study of single stars or well-separated component stars in a binary because the surface magnetic structures responsible for most of the Ca II emission do not migrate in the latitudinal direction, as one would naively assume based on experience from the solar case. The reason is that the participation of helicity in dynamo action is substantial only in the heated region, and the field is simply being wound up outside of this region. We note that such a scenario of binary interaction is not entirely irrelevant to our preliminary study of some of the active late-type stars in Section 5.

We note that the well-known and pronounced equatorward propagation of the dynamo wave for the case of the Sun is specific to sunspots, while other tracers of solar activity can be interpreted as an activity cycle pattern suggesting the presence of a standing wave. In particular, Obridko & Shelting (2003) derived and analysed the solar butterfly diagram for large-scale surface magnetic field. This tracer is associated with the poloidal component of the dynamo-generated magnetic field while sunspots represent the toroidal component. Obridko & Shelting (2003) found that the latitudinal migration is much less pronounced for the poloidal field than for the toroidal. Obridko et al. (2004) further supported this conclusion, originally made by naked eye estimates but now based on analyses from a wavelet transform. They explained the differences in the pattern of activity tracers in terms of toroidal and poloidal fields, with the added influence of meridional circulation. In general, meridional circulation is an obvious physical effect that could contribute to the interactions between toroidal and poloidal magnetic fields (see e.g. Dikpati & Gilman 2001; Haber et al. 2002).

The records for late type stars available from the MWO HK Project exhibit magnetic activity patterns on decadal scales that are much more varied than that of the Sun. In this preliminary interpretation of a few patterns, we have moved beyond a straightforward generalization of the solar activity wave propagating from middle latitude towards the

equator, and recognize that stellar magnetic activity may easily include standing dynamo waves or even highly irregular dynamo fields.

Acknowledgements

We acknowledge the dedicated efforts of our many colleagues from the MWO HK Project and thank Steve Keil and Tim Henry of the National Solar Observatory for the AFRL/Sac Peak Ca K-line data series and regular updates. Financial support from the AFSOR under grant AF 49620-02-1-0194 and RFBR under grant 04-02-16094 are noted. The work of W.S. is also partially supported by American Petroleum Institute Grant No. 2004-101274.

REFERENCES

Baliunas S. L., Donahue R. A., Soon W. et al., 1995, ApJ, 438, 269.

Baliunas, S, Frick, P., Moss, D., Popova, E., Sokoloff, D., Soon, W.: 2004, Sol. Phys., 224, N 1-7, 179

Bassom A., Kuzanyan, K., Soward, A.M.: 1999, Proc. Roy. Soc. Lond., A454, 1283.

Covas, E., Moss, D., Tavakol, R.: 2005, A&A, 429, 657.

Dikpati, M., Gilman, P. A.: 2001, ApJ, 559, 428.

Donahue, R. A., Baliunas, S.L., Frazer, J., French, H., Lanning, H.: 1986. In Zeilik, M. and Gibson, D.M. (Eds), The Fourth Cambridge Workshop on Cool Stars, Stellar Systems and the Sun, Springer, 281.

Fawzy, D., Stepien, K., Ulmschneider, P., Rammacher, W., Musielak, Z.F.: 2002a, A&A, 336, 994.

Fawzy, D., Ulmschneider, P., Stepien, K., Musielak, Z.E., Rammacher, W.: 2002a, A&A, 336, 983.

Frick, P., Galyagin, D., Hoyt, D., Nesme-Ribes, E., Shatten, K., Sokoloff, D., Zakharov, V.: 1997, A&A, 328, 670.

Frick, P., Soon, W., Popova, E., & Baliunas, S.: 2004, New Astron., 9, 599.

Galitski, V.M., & Sokoloff, D.D.: 1999, Geophys. Astrophys. Fluid Dynamics, 91, 147.

Haber, D.A., Hindman, B.W., Toomre, J., Bogart, R.S., Larsen, R., Hill, F.: 2002, ApJ, 570, 855.

Kraft, R.P.: 1967, ApJ, 150, 551.

Krause, F. & Rädler, K.-H.: 1980. Mean-Field Magnetohydrodynamic and Dynamo Theory. Pergamon Press.

Meunier, N., Proctor, M.R.E., Sokoloff, D., Soward, A.M., Tobias, S.: 1997, Geophys. Astrophys. Fluid Dyn., 86, 249.

Mohanty, S., Basri, G.: 2003, ApJ 585, 451.

Moss, D., Piskunov, N., Sokoloff, D.: 2002, A&A, 396, 885.

Moss, D., Sokoloff, D., Kuzanyan, K., Petrov, A.: 2004, Geophys. Astrophys. Fluid Dyn., 98, 257.

Obridko, V.N., Shelting, B.D.: 2003, Astron. Rep., 47, 333.

Obridko, V.N., Sokoloff, D.D., Kuzanyan, K.M., Shelting, B.D., Zakharov, V.G., Proceedings of JENAM Meeting 2004, in press.

Parker, E.: 1955, ApJ, 122, 293.

Schekochihin, A.A., Cowley, S.C., Taylor, S.F., Maron, J.L., McWilliams, J.C.: 2004, ApJ 612, 276.

Sokoloff, D., Nesme-Ribes, E.: 1994, A&A 288, 293.

Soon, W., Frick, P., Baliunas, S.: 1999, ApJL 510, L135.

Strassmeier, K.G.: 2005, Astron. Narchr., 326, 1.

Suchkov, A.A., Makarov, V. V., Voges, W.: 2003, ApJ, 595, 1206.

Wilson, O.C.: 1978, ApJ, 226, 329.

Wilson O. C.: 1963, ApJ, 138, 832.

Zeldovich, Ya. B., Ruzmaikin, A. A., Sokoloff, D. D.: 1990, The almighty chance, World Sci., Singapore.

This manuscript was prepared with the AAS LaTeX macros v5.2.

Table 1: Two measures of the anharmonicity of stellar cycles (see text for explanation) for different stars ("y" denotes a young star) derived from recorded daily Ca II H and K time series of the Mount Wilson HK Project as studied earlier in Frick et al. (2004) and preliminarily reported in Baliunas et al. (2004). The record for the Sun is from the Sacramento Peak Observatory (S. Keil and T. Henry, private communication).

Object	P_c (years)	A	M_2/M_1
HD 16160	12.3	1.0	0.02
HD 146233	8	1.0	0.14
HD 26913 (y)	5.8	1.0	0.17
HD 160346	7.1	1.2	0.03
HD 161239	5.1	1.3	0.02
HD 10476	10.4	1.3	0.16
HD 4628	8.5	1.4	0.02
Sun	11	1.5	0.03
HD 81809	8.1	1.5	0.08
HD 26965 (y)	10	1.5	0.18
HD 103095	7.2	1.5	0.18
HD 187691	8	1.7	0.08
HD 219834B	16	1.7	0.15
HD 20630 (y)	5.5	2.9	0.11
HD 18256(y)	7	3.8	0.27

Table 2: Anharmonicity measures, A and M_2/M_1, for solutions of the Parker migratory dynamo ($D_\odot = -10^3$ and $\mu_\odot = 3$). Where two entries are shown, the one at left is A value, and at right is M_2/M_1 value.

$D/D_\odot$	$\mu/\mu_\odot$				
	0	0.1	0.5	1.0	2.0.
0.1	decays	decays	decays	decays	decays
0.3	1.48/0.05	1.13/0.04	0.93/0.01	decays	decays
1	1.58/0.11	1.53/0.08	1.51/0.06	1.1/0.001	decays
10	1.56/0.16	1.59/0.15	1.62/0.25	1.49/0.002	0.94/0.001
100	1.5/0.18	1.56/0.16	1.84/0.36	1.65/0.57	0.96/0.003
1000	1.57/0.21	1.58/0.15	5.13/1.22	aperiodic	0.9/0.01

Table 3: Testing for robustness of the anharmonicity measures allowing for potential hemispheric bias-induced phase shifted signals (as expressed in Eq. [6]) artifically introduced into the Parker migratory dynamo ($D_\odot = -10^3$ and $\mu_\odot = 3$) solutions of Moss et al. (2004).

τ	$c = 1$		$c = 1.5$	
	A	M_2/M_1	A	M_2/M_1
	$D/D_\odot = 100$, $\mu/\mu_\odot = 0.1$			
0	1.56	0.17	1.56	0.16
0.05	1.56	0.15	1.56	0.15
0.1	1.51	0.12	1.56	0.12
0.15	1.51	0.07	1.51	0.08
0.2	1.39	0.03	1.56	0.03
	$D/D_\odot = 1000$, $\mu/\mu_\odot = 0.5$			
0	5.13	1.22	5.13	1.22
0.05	3.89	1.13	3.39	1.01
0.15	6.4	0.53	6.4	0.44
0.2	4.99	0.18	5.13	0.22
0.25	4.23	0.0002	4.35	0.08
	$D/D_\odot = 10$, $\mu/\mu_\odot = 1.0$			
0	1.47	0.027	1.47	0.027
0.05	1.47	0.024	1.47	0.022
0.1	1.47	0.018	1.47	0.018
0.15	1.43	0.011	1.43	0.001
0.2	1.32	0.0025	1.39	0.004
0.25	0.92	0.00005	1.44	0.002
	$D/D_\odot = 100$, $\mu/\mu_\odot = 1$			
0	1.65	0.52	1.65	0.5
0.05	1.65	0.50	1.65	0.5
0.1	1.56	0.38	1.56	0.4
0.15	1.52	0.24	1.52	0.3
0.2	1.47	0.08	1.52	0.1
0.25	2.0	0.0006	1.69	0.04

Table 4: Summary of properties of dynamo waves for the Parker migratory dynamo ($D_\odot = -10^3$ and $\mu_\odot = 3$). "M" denotes a migratory pattern, "SW" a standing wave and "I" an intermediate form.

$D/D_\odot$	$\mu/\mu_\odot$					
	0	0.1	0.5	1.0	2.0	2.5.
0.1	decays	decays	decays	decays	decays	decays
0.3	I	I	M	decays	decays	decays
1	SW	SW	M	M	decays	decays
10	SW	SW	SW	M	M	M
100	SW	SW	SW	I	M	M
1000	SW	SW	SW	aperiodic	I	M

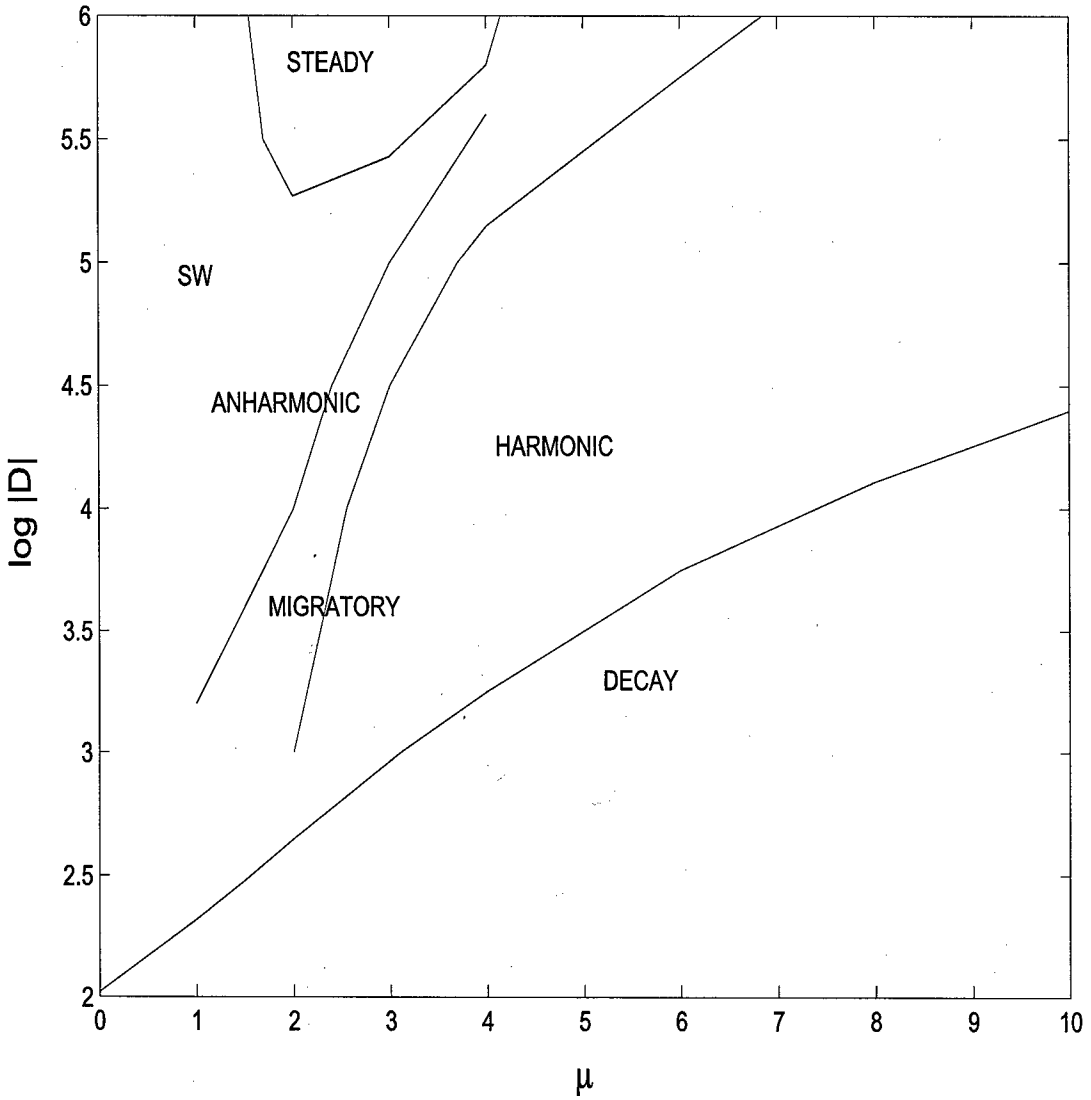

Fig. 1.— Qualitative mapping of dynamo solutions as functions of μ and D for the α-quenching of the form in (5). The symbol "SW" denotes standing wave solutions.

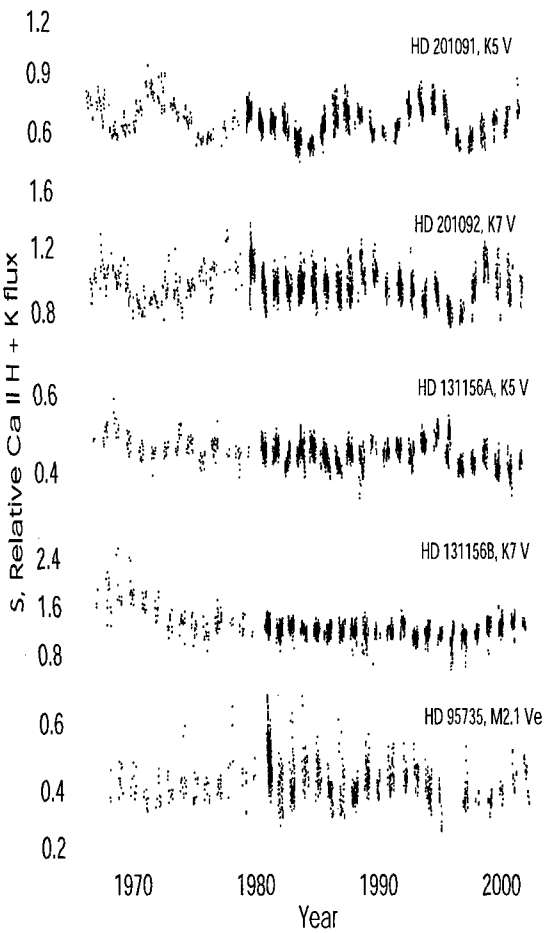

Fig. 2.— Ca II H and K chromospheric activity time series for five stars: a) HD 201091; b) HD 201092; c) HD 131156A; d) HD 131156B; e) HD 95735. The signals on the vertical axes are given in arbitrary units, common for all stars presented.

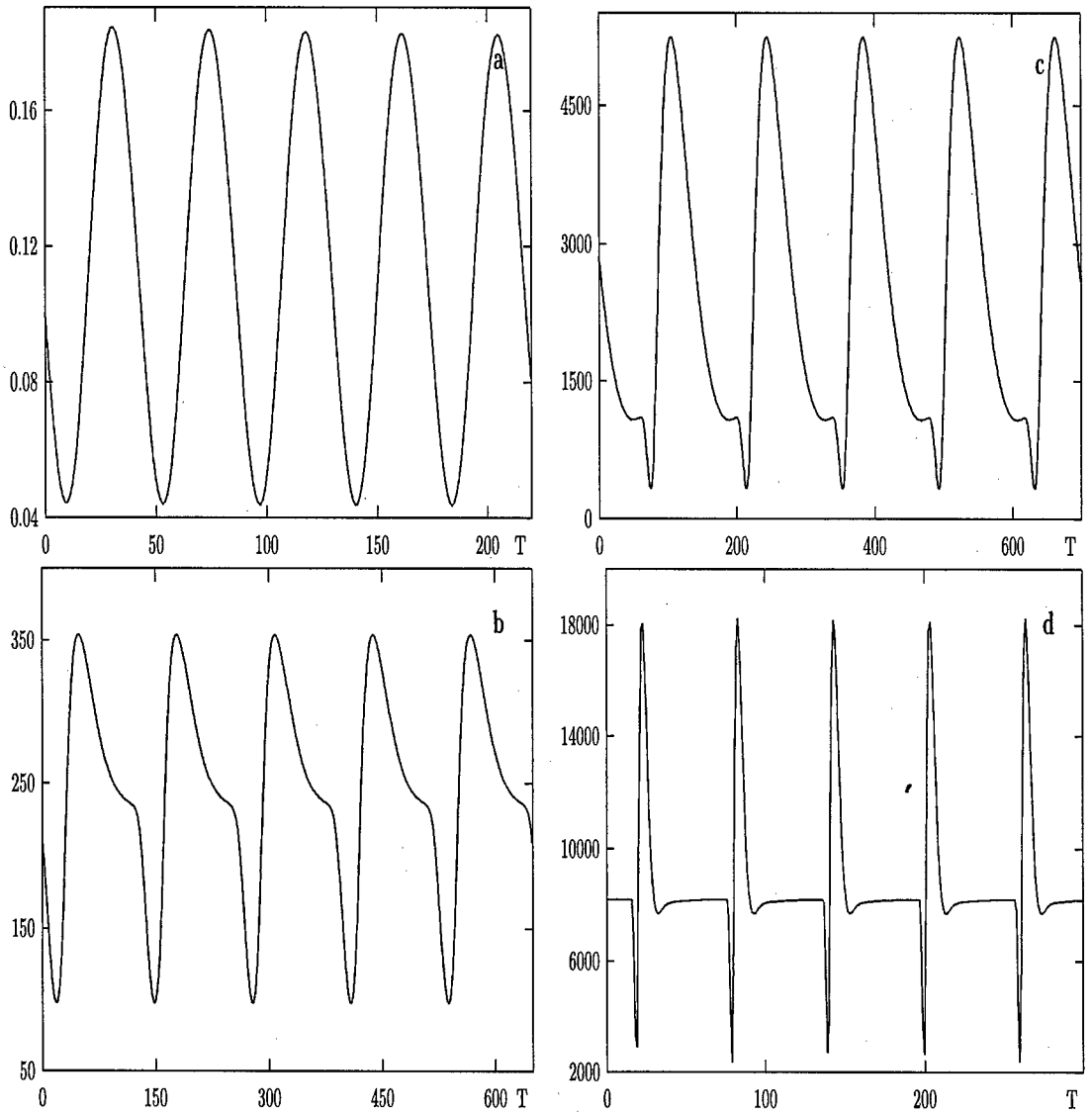

Fig. 3.— Time series from numerical simulations of the Parker migratory dynamo model: a) $D = -10^3, \mu = 3$; b) $D = -10^5, \mu = 3$; c) $D = -10^5, \mu = 1.5$; d) $D = -10^6, \mu = 1.5$. The magnetic field on the vertical axes is given in units of the equipartition field strength, and the time T is given in units of the diffusion time.

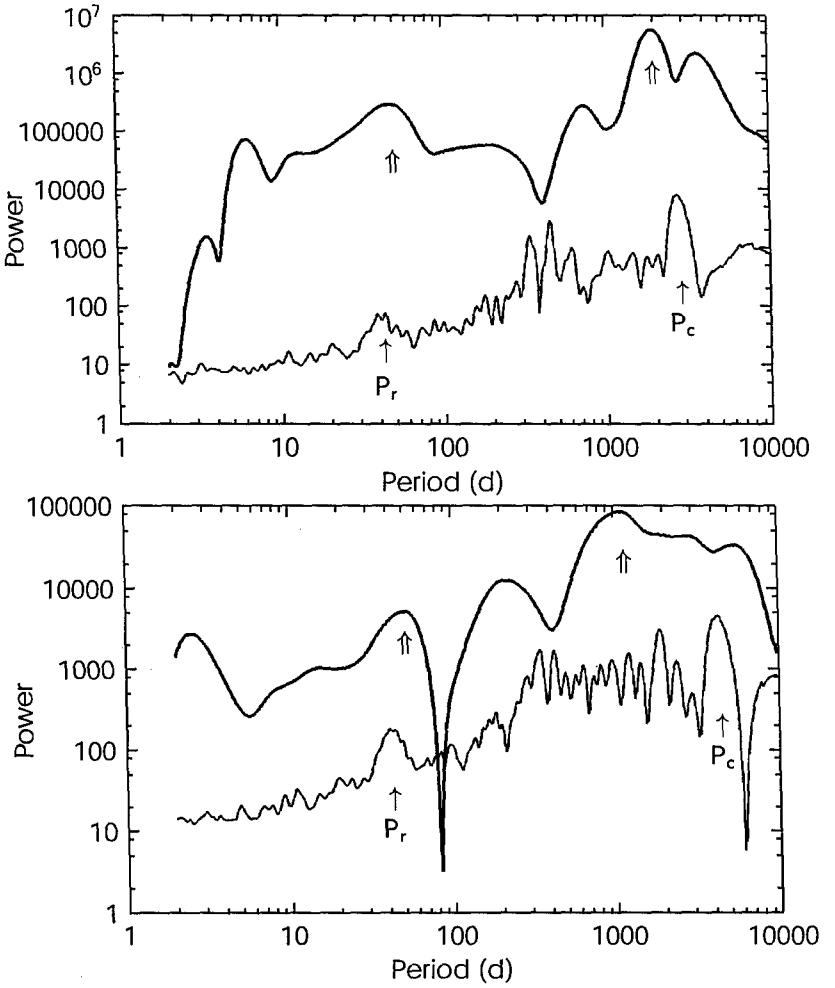

Fig. 4.— Wavelet and DWA spectra, shown as thin and thick solid lines, respectively, for both (a) HD 201091 and (b) HD 201092. The wavelet and DWA spectra were calculated using $\kappa = 4$ which produce smoother peaks than corresponding Fourier transform results (i.e. $\kappa \rightarrow \infty$) that in turn allow their application to quantify anharmonicity of stellar activity cycles. Thin arrows marked with P_r and P_c for the wavelet spectra denote the identifiable rotation and interannual cyclic periods while broad, unmarked arrows in the DWA spectra pinpoint either the re-tuned rotation peaks or shifted interannual cyclic scale, a^*, for quantification of anharmonicity. Vertical scale for the DWA spectra are shifted vertically by an arbitrary amount to avoid overlapping with the wavelet spectra.

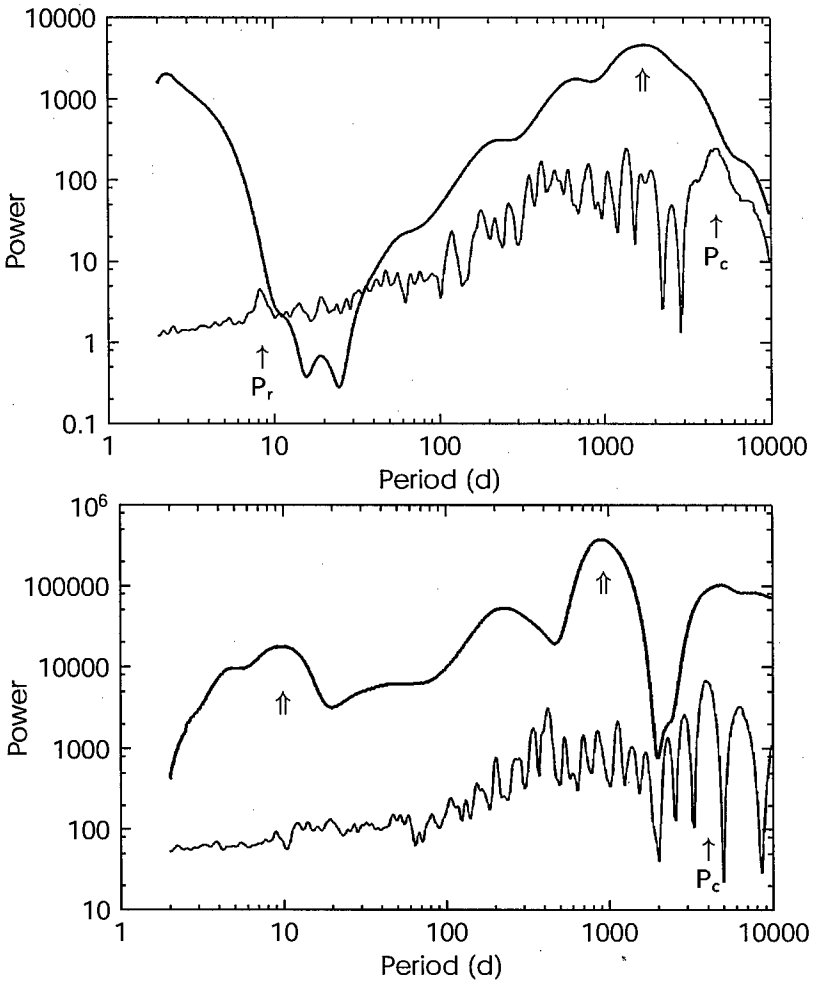

Fig. 5.— Wavelet and DWA spectra for (a) HD 131156A and (b) HD 131156B. Notation as in Fig. 4.

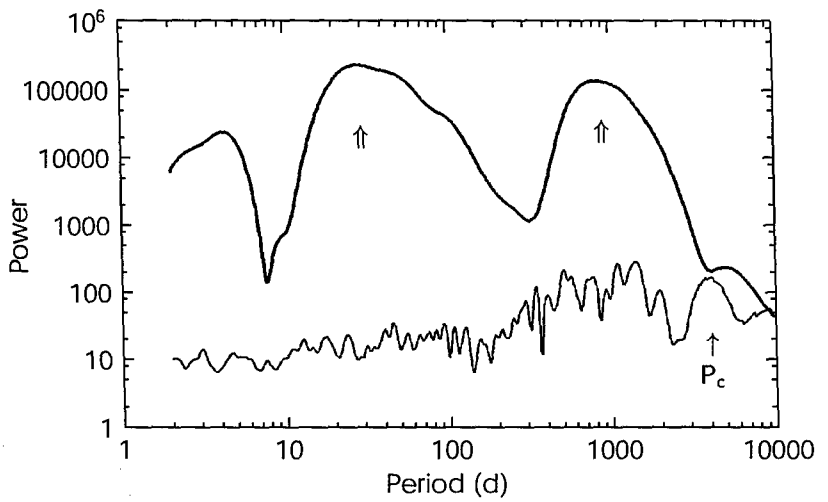

Fig. 6.— Wavelet and DWA spectra for HD 95735. Notation as in Fig. 4.

AFFARS Part 5349

PAGE < | TOC | HOME | PAGE >

LIBRARY

LIBRARY

Laws / Regulations / Policy	Informational Guidance	Training	Community Advice	Suggestion Box

PART 5349
Termination of Contracts
[Revised 4 AUG 2004]

SUBPART 5349.4 — TERMINATION FOR DEFAULT

5349.402 Termination of fixed-price contracts for default. (No Text)

5349.402-3 Procedure for default.

(d) For all ACAT I, II, and III Programs, the contracting officer shall, upon issuance of the cure notice, immediately inform SAF/AQCK and forward a copy of the cure notice to SAF/AQCK. In addition to ACAT program notices, contracting officers shall notify SAF/AQCK of any other notices that could result in high-level Air Force interest.

(e)
(1) For all ACAT I, II , and III Programs, the contracting officer shall, upon issuance of the show cause notice, immediately inform SAF/AQCK and forward a copy of the show cause notice to SAF/AQCK. In

addition to ACAT program notices, contracting officers shall notify SAF/AQCK of any other notices that could result in high-level Air Force interest.

(f) Prior to making a final decision concerning termination for default, the contracting officer shall forward the termination notice and the complete contract file to AFMCLO/JAB and follow the procedures in 5333.291(b).

(h) For termination notices related to ACAT I, II, and III Programs, the contracting officer shall, upon issuance of the termination notice, immediately inform SAF/AQCK and distribute a copy of the termination notice to SAF/AQCK. In addition to ACAT program notices, contracting officers shall notify SAF/AQCK of any other notices that could result in high-level Air Force interest.

5349.402-6 Repurchase against contractor's account.

The contracting officer shall provide copies of assessments of excess reprocurement costs to DFAS/BKRD/CC and AFMCLO/JAB.

5349.403 Termination of Cost-Reimbursement Contracts for Default

(a) For all ACAT I, II, and III Programs, the contracting officer shall, upon issuance of the termination notice, immediately inform SAF/AQCK and forward a copy of the termination notice to SAF/AQCK. In addition to ACAT program notices, contracting officers shall notify SAF/AQCK of any other notices that could result in high-level Air Force interest.

SUBPART 5349.5 — CONTRACT TERMINATION CLAUSES

5349.501-70 Special termination costs.

(a) Contracting officers shall refer to Volume 2A, Chapter 1, Section 010213, paragraph C.2 of DoD 7000.14-R, DoD Financial Management Regulation, for Congressional notification and additional approval requirements for Special Termination Cost Clauses (STCCs). Because STCCs require special notification to Congress and entail a long approval process over which the Air Force has little control, the contracting officer should allow SAF/AQCK sufficient time to process requests to use DFARS 252.249-7000, Special Termination Costs (i.e. not less than 90 days prior to contract award). The request shall include the following:

(i) A detailed breakdown of applicable cost categories in the clause at DFARS 252.249-7000 (a) (1) through (5), which includes the reasons for the anticipated incurrence of the costs in each category;

(ii) Information on the financial and program need for the clause including an assessment of the contractor's financial position and the impact of a failure to receive authority to use the clause; and

(iii) Clear evidence that only costs that arise directly from a termination would be compensated under the clause. Costs that would be incurred by the Government, regardless of whether a termination occurs, shall not be covered by a STCC.

(c) The contracting officer shall obtain SAF/FM approval prior to authorizing any increase in the Government's maximum liability under the clause.

SUBPART 5349.70 — SPECIAL TERMINATION REQUIREMENTS

5349.7001 Congressional notification on significant contract terminations.

(c) The contracting officer shall submit the request for clearance to SAF/AQCK at least five work days before the proposed termination date. SAF/AQCK will forward the clearance request to SAF/LLP. The contracting officer shall not release the termination notice until SAF/LLP contacts the contracting officer, indicating the date and time that Congress will be notified and the contractor should receive the termination notice.

(d)(5) "Contract price of the items terminated" means the contract price of the supplies or services not yet accepted that are being terminated. The contracting officer shall not adjust this amount downward for progress or advance payments, accepted vouchered costs, or less than full funding and should use estimates when unpriced contract actions are being terminated, or when otherwise necessary.

PAGE < | TOP ^ | TOC ≡ | HOME ⌂ | PAGE >

AFRL SES PERFORMANCE TIMELINE

31 Jul 05	SES feedback completed (Ratee Self-Assessment and Rater)
4 Aug 05	AFRL/CD issues instructions and provides hard copy of Senior Leader Evaluation Form to SES members and/or rater
16 Aug 05	SES members provide draft hard copy of Senior Leader Evaluation Form remarks/accomplishments, and proposed rater and reviewer comments to AFRL/DP
	AFOSR SES members submit all documentation through Dr. Godfrey
18 Aug 05	AFRL/DP will compile data and provide hard copies of Senior Leader Evaluation Form remarks/accomplishments and proposed rater and reviewer comments to AFRL/CC
1 Sep 05	AFRL/CC completes "draft" evaluation in P&DMS Rank, 1-n
6-12 Sep 05	AFRL/CC loads final ratings into P&DMS
15 Sep 05	All evaluations need to be loaded into the system
End Sep 05	AFMC Panel
14-16 Nov 05	AF Performance Review Board (PRB) meets
Jan 06	Pay raises implemented and performance incentives paid out